Phys. Status Solidi B **252,** No. 8, 1792–1798 (2015) / **DOI** 10.1002/pssb.201451607

physica status solidi b
www.pss-b.com
basic solid state physics

Magnetoresistance effect in anion-substituted manganese chalcogenides

S. S. Aplesnin[1,2], O. B. Romanova[*,1], and K. I. Yanushkevich[3]

[1] Kirensky Institute of Physics SB RAS, Akademgorodok 50, Krasnoyarsk 660036, Russia
[2] Siberian State Aerospace University M F Reshetnev, Krasnoyarsky Rabochy Av. 31, Krasnoyarsk 660014, Russia
[3] Scientific-Practical Materials Research Center NAS, P. Brovski Str.19, Minsk 220072, Belarus

Received 7 October 2014, revised 3 February 2015, accepted 20 February 2015
Published online 19 March 2015

Keywords electron tunneling, magnetic properties, magnetoresistance, semiconductors

[*] Corresponding author: e-mail: rob@iph.krasn.ru, Phone: +391 2907108, Fax: +391 2438923

The electric and magnetic properties of anion-substituted antiferromagnetic $MnSe_{1-x}Te_x$ ($0.1 \le x \le 0.4$) semiconductors in the 77–700 K temperature range and magnetic fields under 1 T are studied. In the $MnSe_{1-x}Te_x$ solid solutions, negative magnetoresistance in the vicinity of the Néel temperature for $x = 0.1$ and for composition with $x = 0.2$ in the paramagnetic range below 270 K is revealed. A dependence of the magnetic susceptibility versus the prehistory of the samples is found. The model of localized spin-polarized electrons with the localization radius depending on the magnetic field is proposed for $x = 0.1$. In the paramagnetic range, the negative magnetoresistance and the behavior of magnetic moment are a result of orbital glass formation.

1 Introduction Chalcogenides are widely used in technical devices and the chemical engineering industry, primarily because they provide almost all known types of magnetic ordering and electrical conductivity. Many chalcogenides are good model systems for technical devices based on the physical phenomena such as metal–insulator transition and the magnetoresistance effect [1–3]. Manganese oxide compounds ($LaMnO_3$-type manganites) [4–8], europium chalcogenides, $CdCr_2Se_4$, $Cd_{1-z}Mn_zTe_{1-y}Se_y$, $HgCr_2Se_4$ selenides, and sulfides [9–13] are intensively studied. In sulfide systems $Me_xMn_{1-x}S$ (Me = 3d, 4f metal), the metal–insulator transition and a colossal magnetoresistance (GMR) effect are revealed. The value of GMR is comparable to that of manganites [14–17].

The manganese chalcogenides MnSe and MnTe are antiferromagnetic (AFM) compounds with transition temperature increasing with molecular weight [18–20]. Manganese monoselenide, MnSe, manifests a structural phase transition from a cubic phase to an NiAs structure in the $248\ K < T < 266\ K$ temperature range [21], and the phases coexistence in the sample are observed below a temperature of 248 K. The magnetic phase-transition temperature, as derived from neutron diffraction studies [22], is $T_N = 135$ K for MnSe in the cubic modification, while in the hexagonal NiAs phase it coincides with the temperature of the structural transition $T_S \sim 270$ K.

On the other hand, MnTe crystallizes in hexagonal NiAs type structure with metallic conductivity [20, 23, 24]. Antiferromagnetic MnTe consists of ferromagnetically ordered spins in the planes, which are oriented antiferromagnetically along the hexagonal axis. The spins are located in the basal plane and have easy-plane anisotropy with the Néel temperature $T = 310$ K [25]. The rise in susceptibility below 83 K could be explained to be due to a magnetoelastic coupling that strengthens intraplanar ferromagnetic interactions relative to interplanar antiferromagnetic interactions [26].

The electronic structure of MnB^{VI} (B^{VI} = S, Se, Te) has been investigated by using the LDA + U method [27]. All these MnB^{VI} compounds have semiconducting electronic structure in the antiferromagnetic phase. The character of each energy gap is on the crossroads between charge-transfer-type insulators and band insulators. The LDA + U method yields enhanced energy gaps and magnetic moments, as compared to those of the LDA calculation in agreement with experimental. The energy gap in the spectrum of single-particle electron exitations is 2.0–2.5 eV for MnSe and 0.9–1.3 eV for MnTe. Manganese chalcogenides reveal p-type conductivity. The magnetoresistance

effect in the magnetically ordered cubic phase MnSe is revealed near the Néel temperature with the specific electrical resistivity value $\rho = 10^4$–$10^3\,\Omega\,\mathrm{cm}$ [28]. Reduction of the bond length of the Mn–Te metal–anion, according to theoretical calculations of the band structure [19], induces a change in crystal structure from cubic to hexagonal type with antiferromagnetic ordering type and a binding energy per Mn–Te pair $E_{ZB,H} = -0.31$ eV/bond with bond length $R_{AF} = 2.70$ Å and with ferromagnetic ordering $E_{ZB,H} = -0.51$ eV/bond with $R_F = 2.71$ Å. The lattice constant $a = 0.546$ nm in MnSe with NaCl structure is also decreased on cooling. The thermal expansion coefficient is 2.4×10^{-5} 1/K for $x = 0.2$ [29]. On cooling the constant lattice is decreased and tends to $a = 0.542$ nm at the Néel temperature. So, the substitution of selenium by tellurium at low concentrations may lead to the formation of ferromagnetic Mn–Te–Mn bonds.

The current carrier is a spin polaron that is localized below the Néel temperature and the conductivity depends on the spin polarization of localized electrons. The change in the transport properties from semiconductor to metal is possible near to room temperature in solid-solution $MnSe_{1-x}Te_x$. Therefore, the appearance of the magnetoresistive effect in anion-substituted $MnSe_{1-x}Te_x$ solid solutions can be expected. Substitution of selenium by tellurium leads to suppression of the hexagonal phase and to a single-phase state of the $MnSe_{1-x}Te_x$ system with FCC structure by $Fm\bar{3}m$ (225) space group [30] in the $120\,\mathrm{K} < T < 300\,\mathrm{K}$ temperature range for compounds with $0.1 \le x \le 0.4$ [29]. Random local deformations of the lattice induce a change in the electronic structure and in conductivity with hopping type, together with magnetic property changes.

The aim of this work is the detection of the magnetoresistive effect and to shed light on the microscopic mechanism of the magnetic-field influence on the transport properties of $MnSe_{1-x}Te_x$ ($0.1 \le x \le 0.4$) solid solutions by the comprehensive study of the electrical resistivity and magnetic properties and the current–voltage characteristics as a function of temperature, magnetic field, and concentration.

2 Experimental results and discussion The synthesis of samples in the $MnSe_{1-x}Te_x$ ($0 \le x \le 0.4$) system, with a step in concentration of $x = 0.1$, was performed by the solid-phase reaction method described in Ref. [29] using a step mode. The samples were prepared from powders of electrolytic manganese, with a special purification of the lobes before grinding, as well as selenium and tellurium of special purity grade. The X-ray diffraction patterns of powders of the studied compositions were obtained at room temperature using Cu Kα radiation in the point-by-point measurement mode: the time of collection of information at the point was $\tau = 3$ s, and the angular scan step was $\Delta 2\theta = 0.03^\circ$. X-ray studies show that the anion replacement in the $MnSe_{1-x}Te_x$ system with increase in the tellurium concentration leads to an appreciable change of diffraction reflections intensity toward reduction. Smooth displacement of reflections (422), (420), (331), (400) angular positions on the wide 2θ angles toward smaller values is observed that testifies to an increase in the elementary cell sizes. The reduction of the diffraction reflections intensity on X-ray patterns, most likely, is connected by the fact that the solid-solution formation at replacement especially in anion sublattice is accompanied by essential crystal distortions and growth of cubic structure disorder of the $Fm\bar{3}m$ (225) space group. Despite this, a linear increase of parameter a and an elementary crystal cell of samples with increase in the tellurium concentration allows us to draw a conclusion that in the $0 \le x \le 0.4$ concentration range in the $MnSe_{1-x}Te_x$ system exist solid solutions with space group $Fm\bar{3}m$ (225) structure. The dependence of elementary cell parameter a of $MnSe_{1-x}Te_x$ samples on x concentration is presented in Fig. 1.

Resistivity measurements were carried out by the standard four compensation methods at constant current in the 77–300 K temperature range in magnetic fields up to 1 T. The temperature-dependent conductivity of the $MnSe_{1-x}Te_x$ solid solutions is presented in Fig. 2. All compositions ($0 \le x \le 0.4$) reveal the conductivity typical for semiconductors. At $T < T_N$ there is a deviation from the linear $\ln\sigma = \ln\sigma_0 - \Delta E/T$ dependence. The activation energy ΔE determined from the slope of the linear part of conductivity is equal to $\Delta E \approx 0.07$–0.09 eV and weakly dependent on the composition of these samples.

The influence of magnetic field on the transport properties was investigated by two methods. First, the temperature dependence of the resistance of $MnSe_{1-x}Te_x$ solid solutions was measured both in the magnetic field, and in its absence. Secondly, at a fixed temperature the current–voltage characteristics in a zero magnetic field and in the field $H = 1$ T were studied. Figure 3 presents the current–voltage characteristics for $MnSe_{1-x}Te_x$ manganese chalcogenides with $x = 0.1$ at temperatures of 100, 140, and 190 K. The dependences $U(I)$ are linear and do not depend on the magnetic field at $T = 100$ K. It was established that the

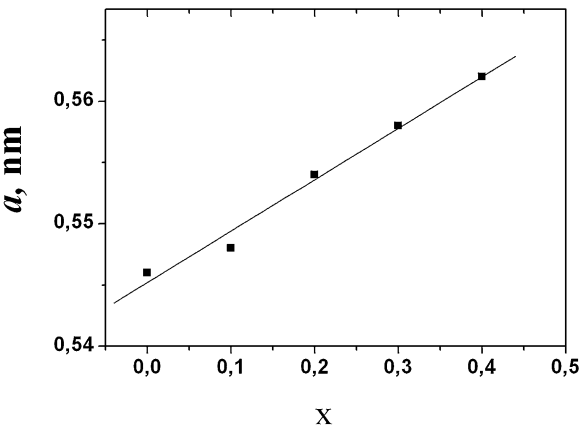

Figure 1 Dependence of elementary cell parameter for the $MnSe_{1-x}Te_x$ system.

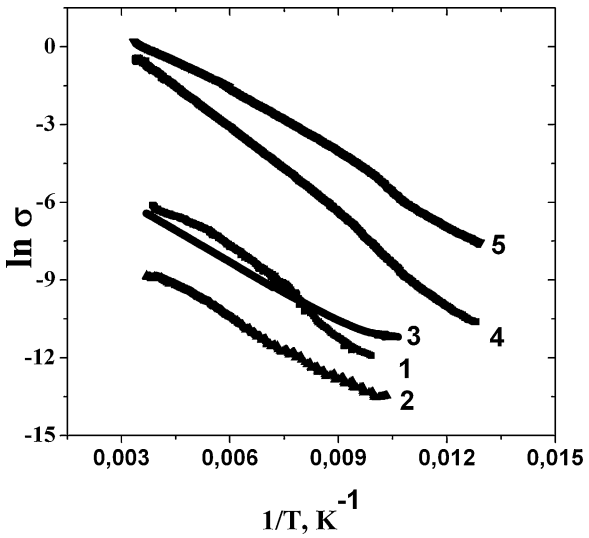

Figure 2 The temperature dependence of the conduction for $MnSe_{1-x}Te_x$ solid solutions with $x = 0$ (1), 0.1 (2), 0.2 (3), 0.3 (4), 0.4 (5).

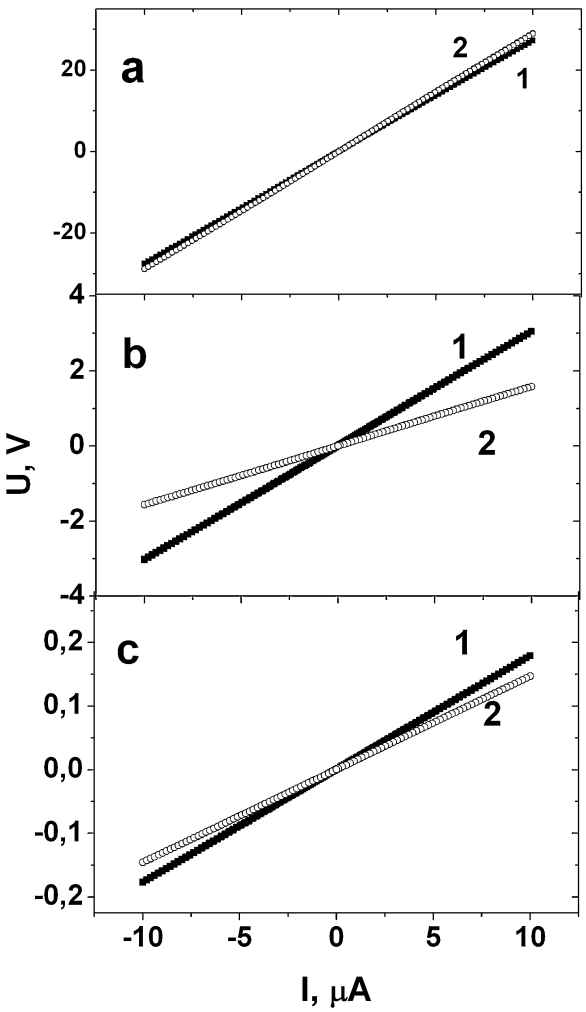

Figure 3 Current–voltage characteristics of the $MnSe_{0,9}Te_{0,1}$ solid solution in magnetic field $H = 1$ T (2) and in zero magnetic field (1) at different temperatures T: 100 K (a), 140 K (b), 190 K (c).

resistance of the samples decreases in a magnetic field and the greatest change, of the order of 100% was detected in the vicinity of the Néel temperature for composition with $x = 0.1$ (Fig. 4). Decreasing resistance was found in the paramagnetic range at $160\,\mathrm{K} < T < 270\,\mathrm{K}$ above the Néel temperature for concentration $x = 0.2$ (Fig. 4b). The magnetoresistance $\delta_H = (\rho(H) - \rho(0))/\rho(0)$ in $MnSe_{1-x}Te_x$ was not revealed for higher concentrations. The inset in Fig. 4 shows the temperature dependence of the magnetoresistance for monoselenide manganese in a magnetic field of 0.45 T. For MnSe the magnetoresistive effect is observed at temperatures below the Néel temperature [21]. The temperature dependence of the resistivity for compounds MnTe in different magnetic fields ($H = 0$, 1, 1.5 T) does not establish the magnetic-field influence on the electrical resistivity. Measurement of the samples magnetic moment was carried out in a magnetic field of 0.86 T in the $80\,\mathrm{K} < T < 700\,\mathrm{K}$ temperature range in two ways: cooling in zero magnetic field (ZFC) and cooling in a magnetic field (FC) $H = 0.86$ T (Fig. 5). The slight growth in magnetization at $T = 340$ K was caused by the formation of nanoareas of a hexagonal phase that is not defined by X-ray methods and disappears on annealing for $x = 0.1$.

Magnetization of a sample cooling in a magnetic field has a smaller value than that of a sample cooling in a zero field. The relative changes of the magnetic moment $\delta_M = (M_{FC} - M_{ZFC})/M_{ZFC}$ are shown in Fig. 5 (inset) and are in qualitative agreement with the temperature behavior of the magnetoresistance. For $x = 0.1$, the relative change of the magnetic moment defined without accounting for the magnetic contribution from the hexagonal phase is increased sharply in the vicinity of the Néel temperature and is decreased in absolute value at $T = 210$ K, where the magnetoresistance disappears. Quantitative agreement between the temperature dependence of the relative change of the moment and magnetoresistance versus the temperature is observed for composition with $x = 0.2$.

The temperature dependences of the susceptibility [29] exhibit maxima that are associated with an antiferromagnetic phase transition in the $MnSe_{1-x}Te_x$ compounds. The Néel temperature of the samples smoothly decreases from 132 K for $MnSe_{0.9}Te_{0.1}$ to 118 K for $MnSe_{0.6}Te_{0.4}$ (Fig. 6). The paramagnetic Curie temperature (θ), determined from the high-temperature region of the inverse susceptibility, is also decreased with increasing tellurium concentration (Fig. 6). MnSe has a second type of magnetic ordering, where the magnetic transition temperature T_N is determined by the exchange interaction in the second coordination sphere (J_2) $T_N = 2/3S(S+1)Z_2J_2$ ($Z_2 = 6$). The paramagnetic Curie temperature is determined by two exchanges J_2, J_1 is exchange between nearest-neighbor exchange and the form is $\theta = 2/3S(S+1)[Z_1J_1 + Z_2J_2]$. Substitution of selenium by tellurium leads to change in three bonds (J_2). The Néel temperature for $MnSe_{1-x}Te_x$ compounds can be

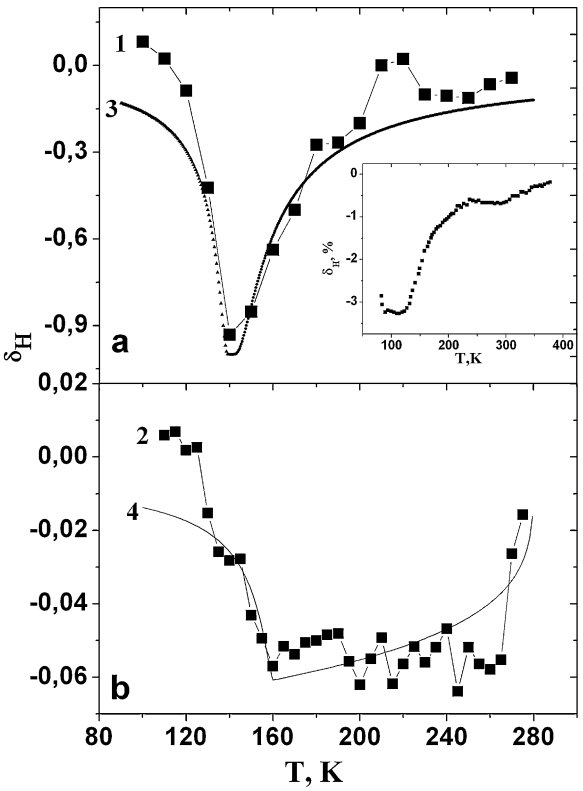

Figure 4 Magnetoresistance $\delta_H = (\rho(H)–\rho(0))/\rho(0)$ temperature dependence of the $MnSe_{1-x}Te_x$ chalcogenides with $x = 0.1(1)$ (a) and 0.2(2) (b) under $H = 1$ T. Fitting functions for concentration $x = 0.1$ (3) from Eq. (1) under $H = 0.8$ T, $B = 0.13$ T^{-1} in the region $T > T_N$, and $B = 0.05$ T^{-1} in $T < T_N$; for $x = 0.2(4)$ from Eq. (5) with parameters $T_0 = 280$ K, $T^* = 160$ K, $n = 2/3$, $\lambda = 0.1$, concentration of clusters $x = 0.08$. Inset: The temperature dependence of the magnetoresistance for MnSe.

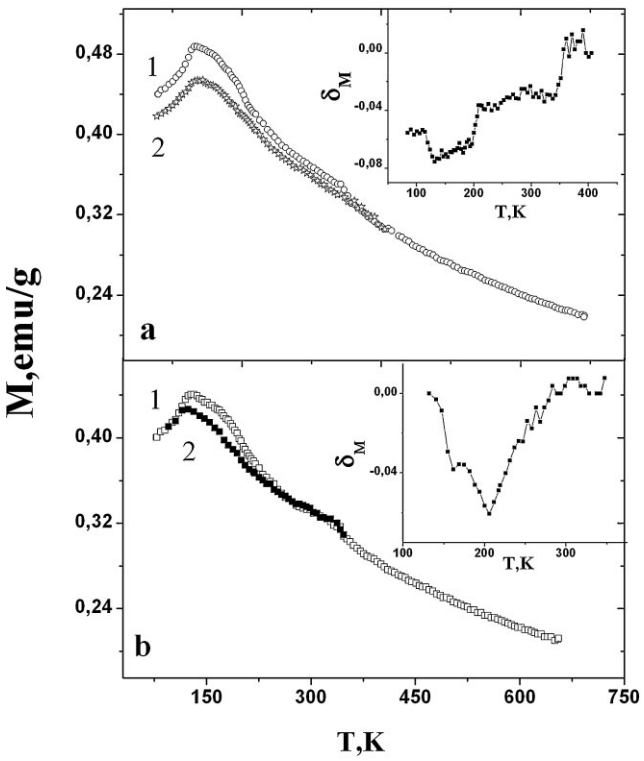

Figure 5 The temperature dependence of the magnetization: (1) cooling at zero magnetic field (ZFC) and (2) measured on cooling of samples in a magnetic field of 0.8 T (FC) for composition $x = 0.1$ (a) and $x = 0.2$ (b). Inset: The temperature dependence of the relative change of the magnetic moment $\delta_M = (M_{FC}–M_{ZFC})/M_{ZFC}$ for the same compositions.

written as $T_N(x) = 2/3S(S+1)[3J_{2,Se}(1–x) + 3J_{2,Te}x + 3J_{2,Se}]$ for small concentration $x \ll 1$. As a result of the independence of the Néel temperature on concentration for $x = 0$ and $x = 0.1$ the exchange interaction in the second coordination sphere does not change on substitution.

For small concentrations, the paramagnetic Curie temperature can be represented as $\theta = 2/3S(S+1)\{Z_1[J_{1,Se}(1–x) + J_{1,Te}\ x] + Z_2J_2\}$. The normalized dependence $\theta(x)/\theta(MnSe) = 1–0.5x(1–J_{1,Te}/J_{1,Se})$ is used to determine the sign of the exchange $J_1(Mn–Te–Mn) = –0.1J_1(Mn–Se–Mn)$ (see Fig. 6).

3 Theoretical model Anionic substitution induces the chemical pressure that leads to an increase in the octahedron crystal field as a result of the difference in the ionic radii of selenium and tellurium. The growth of the crystal-field splitting gives rise to rearrangement of the electron density between t_{2g} and e_g orbitals, i.e., to the transition of electrons from e_g orbital to t_{2g} orbital and to a change in the spin state of the manganese ions in the vicinity of tellurium ions at low concentrations. The sign of the exchange interactions will change, as a result of the appearance of the kinetic exchange in the electron subsystem. Distortion of the octahedron induces the splitting of t_{2g} orbitals with different orbital momentum projection $\pm L^z$ on the selected axis. Orbital ordering can cause condensation of the polar mode, for example, an octahedral rotation mode in the 200–250 K temperature range. To explain the experimental results we suppose formation of ferromagnetic clusters in the vicinity of tellurium ions with

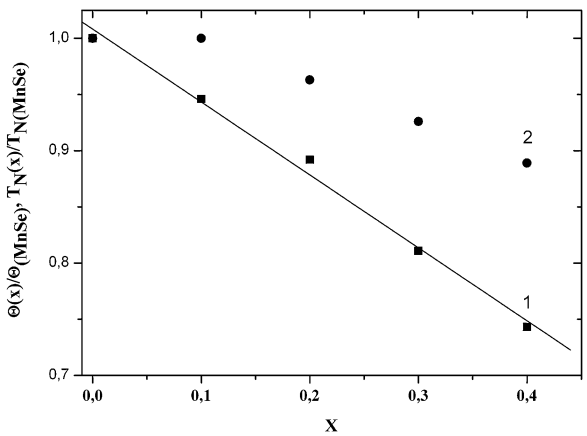

Figure 6 Concentration dependence of the paramagnetic Curie temperature (1) and Néel temperature (2).

random orientation of the anisotropy axes and orbital moments. Two temperature ranges can be chosen in $MnSe_{1-x}Te_x$ solid solution for $x=0.1$ in the vicinity of the Néel temperature and for $x=0.2$ in the paramagnetic region above the Néel temperature. For composition with $x=0.1$, the current carriers are spin-polaron or ferron. In this case the resistivity derivative dR/dT has a maximum near the Néel temperature. The ferron states in antiferromagnetic semiconductors are stabilized by the electron-induced polarization of the ionic crystal lattice [4]. An electron captured by a ferromagnetic microregion polarizes the lattice much more strongly than a free electron and the process reduces the electron energy. The electron–phonon interaction is double the ferron stability. A ferron may exist in a paramagnetic phase at temperatures considerably higher than the Néel temperature.

A competition between electron kinetic energy, polarization of the ionic lattice, and antiferromagnetic exchange interaction of localized spins causes the change in the electron localization radius on temperature.

Magnetoresistance in semiconductors, the conductivity of which is described in the model with variable-range hopping, has an exponential dependence

$$\frac{\rho(H)-\rho(0)}{\rho(0)} = \exp(-BH\xi) - 1 = \exp\left[-\frac{BH}{|1-T/T_N|}\right] - 1, \quad (1)$$

where B is a parameter, H is the external magnetic field, $\xi = 1/|1-T/T_N|$ is the radius of the electron localization [31–34]. Experimental data on the magnetoresistance are satisfactorily described in the framework of this model with field $H=0.8\,T$ and parameter $B=0.13\,T^{-1}$ for $T>T_N$, and $B=0.05\,T^{-1}$ in the magnetically ordered region. Fitting functions are shown in Fig. 4 .

For composition $x=0.2$ the ferromagnetic exchange value is much smaller than the antiferromagnetic interaction one and electrons are localized within the lattice constant in the potential wells, the width of which is fixed and the potential barrier depends on the temperature. In this case the model of spin-polarized electron tunneling between potential wells may be used:

$$\frac{\rho(H)-\rho(0)}{\rho(0)} = \frac{1}{1+xP_1P_2\cos\theta} - 1, \quad (2)$$

where x is the concentration of wells, $P_{1,2}$ is the electron polarization degree, θ is the angle between the axes of electron polarizations. Spin-polarization of electrons is due to orbital ordering. Assume that the polarization values $P_{1,2}$ for all clusters are equal and disappear at the orbital ordering temperature T_0 according to the power law $P_{1,2} = P_0(1-T/T_0)^{1/4}$.

For a qualitative understanding of the processes of electron tunneling between clusters, the polarization axes of which are in the range of angles $0<\theta<\pi$, will consider a simple model. In this model, the anisotropy field H_A is orthogonal to an external magnetic field.

As a result of competition between the Zeeman interaction and anisotropy field, the electron spin (polarization direction) will be turned in the direction of the external magnetic field with increasing temperature. The correlation between the spins is determined by the orbital moments. The magnetic system energy is given by

$$E = -SH\cos\theta - SH_A\cos(\gamma-\theta), \quad (3)$$

where H_A is the anisotropy field, and γ is the angle between the external magnetic field and the anisotropy field. The minimum energy is achieved at an angle:

$$\cos\theta = 1/\sqrt{\left(1+H_A^2\sin^2\gamma/(H+H_A\cos\gamma)^2\right)}. \quad (4)$$

The anisotropy field decreases on heating as a power law $H_A = K(1-T/T^*)^n$, where T^* is the temperature at which the anisotropy field associated with rhombic distortion disappears. The ratio of magnetic field to the anisotropy constant is denoted by $\lambda = H/K$. Then, the dependence of the magnetoresistance versus temperature is represented as

$$\frac{\rho(H)-\rho(0)}{\rho(0)} = \frac{1}{1+\dfrac{xP_0^2(1-T/T_0)^{1/2}}{\sqrt{1+(1-T/T^*)^{2n}/\lambda^2}}}. \quad (5)$$

In Fig. 4b, function (5) describes well the experimental results with parameters $T_0=280\,K$, $T^*=160\,K$, $n=2/3$, $\lambda=0.1$; concentration of clusters is $x=0.08$. The model of electron tunneling between degenerate orbital states explains the magnetoresistance.

The temperature behavior of magnetic susceptibility versus the prehistory of the sample is explained in terms of an orbital glass model. In the presence of the spin and orbital moments interacting by means of a lattice, it is necessary to consider the interaction between them as

$$H = -\sum J_S S_i S_j - \sum_{i,j} 4J_m(S_iS_j)(L_iL_j) - \sum_{i,j} J_L(L_iL_j), \quad (6)$$

where J_S is the magnetic exchange interaction, J_m is the interaction between spin and orbital moments, and J_L is the parameter of interaction between orbital moments. The effective integral of magnetic exchange J_S depends on the orbital correlation $J_S^{ef} = J_S + 4J_m\langle L_iL_j\rangle$. The orbital correlator is increased on cooling in the vicinity of temperature of orbital ordering and correlator is raised also in orbital glass under a magnetic field. The magnetic susceptibility of antiferromagnetic is the inverse of exchange interaction $\chi \sim 1/J_S^{ef}$ and enhancement of orbital correlation in a magnetic field leads to the decrease of magnetic

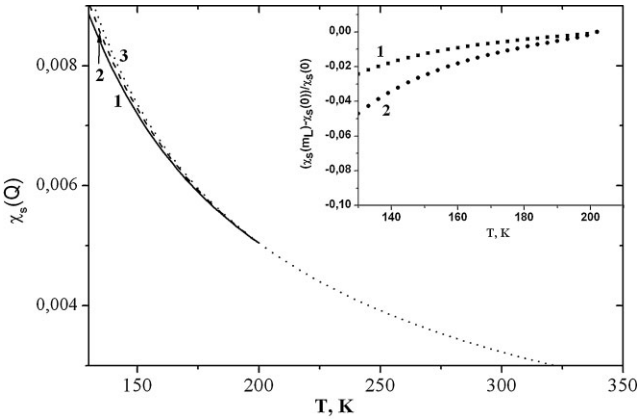

Figure 7 Temperature dependences of the spin susceptibility calculated by Eq. (6) using the parameters $J_S = -135$ K, $J_m = -50$ K, $M_L = m_L(1-T/T_0)^{0.3}$, $T_0 = 210$ K, $m_L = 0$ (3), 0.1 (2), 0.2(1). Inset shows the relative change of the spin susceptibility $(\chi_S(m_L)-\chi_S(0))/\chi_S(0)$ for $m_L = 0.1$ (1) and 0.2 (2).

susceptibility in orbital glass at $J_S < 0$, $J_m < 0$. The total susceptibility can be represented as $\chi = \chi_S + \chi_O + \chi_{SO}$, where χ_S is the magnetic susceptibility of localized spins and χ_O and χ_{SO} are the orbital and mixed susceptibilities, respectively.

Below the temperature of the transition to the orbitally ordered state, the spin and mixed susceptibilities do not obey the Curie–Weiss law and depend on the orbital ordering parameter M_L whose temperature dependence is described by the power-law function. The spin susceptibility at the wave vector of the structure has the form [35]:

$$\chi_s(Q) = \frac{T + J_m(Q)/\left[4(1-4M_L^2)\right]}{T^2 + \frac{T}{4}\left[J_m(Q) - J_S(Q)\right] - 9/\left[4J_mJ_S(1-M_L^2)\right]}, \quad (7)$$

where J_m is the Fourier transform of the exchange integral characterizing the exchange interaction between spin and orbital moments and $J_S(Q)$ is the exchange integral between spins at wave vector $Q = \pi$. The spin susceptibility χ_S is presented in Fig. 7 on the assumption that M_L^2 is proportional to the correlator $\langle L_iL_j\rangle$ that is decreased versus temperature by the power law.

4 Conclusion A magnetoresistance effect of about 100% in the vicinity of the Néel temperature was found in the antiferromagnetic semiconductor $MnSe_{1-x}Te_x$ at the substitution concentration $x = 0.1$. The resistance decreasing in a magnetic field is associated with the increase in the electron localization radius in the potential wells. For $x = 0.2$, a negative magnetoresistance effect in the paramagnetic state, caused by tunneling of the spin-polarized electrons between the orbital states with random orientation orbital moments that are lifted by the external magnetic field, was found. The change of the spin susceptibility in paramagnetic state on cooling of samples in a magnetic field and cooling in zero magnetic fields was found. Such behavior of magnetization is associated with orbital glass arising at high temperature. A correlation between the temperature behaviors of the magnetization and the magnetoresistance of samples was established.

Acknowledgements This study was supported by the official assignment no. 114090470016.

References

[1] S. S. Aplesnin, JETP Lett. **81**, 74 (2005).
[2] A. S. Borukhovich, Physics of the Materials and Structures of the Superconducting and Semiconductor Spintronics (UB RAS, Ekaterinburg, 2004), p. 175.
[3] S. S. Aplesnin, Magnetic and Electrical Properties of Strongly Correlated Magnetic Semiconductors with Four-Spin Interaction and Orbital Ordering (Fizmatlit, Moscow, 2013), p. 176.
[4] E. L. Nagaev, Usp. Fiz. Nauk **166**, 796 (1996).
[5] R. V. Demin, J. O. Gorbenko, A. R. Kaul, L. I. Koroleva, O. V. Melnikov, A. Z. Muminov, R. Szymchak, and M. Baran, Fiz. Tverd. Tela **47**, 2195 (2005).
[6] M. Y. Kagan and K. I. Kugel, Usp. Fiz. Nauk **171**, 577 (2001).
[7] K. I. Kugel, A. L. Rakhmanov, A. O. Sboychakov, M. Y. Kagan, I. V. Brodsky, and A. V. Kloptsov, JETP **125**, 648 (2004).
[8] M. Y. Kagan, A. V. Klaptsov, I. V. Brodsky, K. I. Kugel, A. O. Sboychakov, and A. L. Rakhmanov, Usp. Fiz. Nauk **173**, 877 (2003).
[9] Y. Shapira, S. Foner, N. F. Oliveira, and T. V. Reed, Phys. Rev. B **10**, 4765 (1974).
[10] A. S. Borukhovich, N. I. Ignatieva, A. I. Galyas, S. S. Dorofeichik, and K. I. Yanushkevich, JETP Lett. **84**, 592 (2006).
[11] L. I. Koroleva, R. V. Demin, D. Varchevsky, D. Krok-Kowalsky, T. Midlarz, A. Gilevsky, and A. Pasina, JETP Lett. **72**, 813 (2000).
[12] Z. Yang, S. Tan, Z. Chen, and Y. Zhang, Phys. Rev. B **62**, 13872 (2000).
[13] S. Chehab, J. C. Woolley, A. Manoogian, and G. Lamarche, J. Magn. Magn. Mater. **62**, 312 (1986).
[14] S. Aplesnin, O. Romanova, A. Harkov, D. Balaev, M. Gorev, A. Vorotinov, V. Sokolov, and A. Pichugin, Phys. Status Solidi B **249**, 812 (2012).
[15] S. S. Aplesnin, O. N. Bandurina, O. B. Romanova, L. I. Ryabinkina, A. D. Balaev, and E. V. Eremin, J. Phys. **22**, 226006 (2010).
[16] O. B. Romanova, L. I. Ryabinkina, V. V. Sokolov, A. Y. Pichugin, D. A. Velikanov, D. A. Balaev, A. I. Galyas, O. F. Demidenko, G. I. Makovetskii, and K. I. Yanushkevich, J. Solid State Commun. **150**, 602 (2010).
[17] S. S. Aplesnin, O. B. Romanov, M. V. Gorev, D. A. Velikanov, A. G. Gamzatov, and A. M. Aliev, J. Phys. **25**, 025802 (2013).
[18] J. B. C. Efrem D'Sa, P. A. Bhobe, K. R. Priolkar, A. Das, P. S. R. Krishna, P. R. Sarode, and R. B. Prabhu, Pramana J. Phys. **63**, 227 (2004).

[19] S.-H. Wei and A. Zunger, J. Phys. Rev. B **35**, 2340 (1987).
[20] C. F. Squire, Phys. Rev. **56**, 922 (1939).
[21] K. I. Yanushkevich, Solid Solutions of 3d-Metals Monochalcogenides (A. N. Varaksin, Minsk, 2009), p. 256.
[22] G. I. Makovetskii and A. I. Galyas, Sov. Phys. Solid State **24**, 1558 (1982).
[23] J. J. Allen, G. Luckowsky, and J. C. Mikkelsen, Solid State Commun. **24**, 367 (1977).
[24] J. B. C. Efrem D'Sa, P. A. Bhobe, K. R. Priolkar, A. Das, P. S. Krishna, P. S. Sarode, and R. B. Prabhu, Pramana J. Phys. **63**, 227 (2004).
[25] B. Szuszkiewicz, B. Hennion, B. Witkowska, E. Łisakowska, and A. Mycielski, Phys. Status Solidi C **2**, 1141 (2005).
[26] J. B. C. Efrem D'Sa, P. A. Bhobe, K. R. Priolkar, A. Das, S. K. Paranjpe, R. B. Prabhu, and P. R. Sarode, J. Magn. Magn. Mater. **285**, 267 (2005).
[27] S. J. Youn, B. I. Min, and A. J. Freeman, Phys. Status Solidi B **241**, 1411 (2004).
[28] S. S. Aplesnin, L. I. Ryabinkina, O. B. Romanova, D. A. Balaev, O. F. Demidenko, K. I. Yanuskevich, and H. S. Miroshnichenko, Phys. Solid State **49**, 2080 (2007).
[29] S. S. Aplesnin, O. B. Romanova, M. V. Gorev, A. D. Vasilev, O. F. Demidenko, G. I. Makovetskii, and K. I. Yanushkevich, Phys. Solid State **54**, 1374 (2012).
[30] T. Penkalya, Outlines of Crystallochemistry (Chimia, Leningrad, 1974), p. 496.
[31] N. P. Stepina, E. S. Koptev, A. G. Pogosov, A. V. Dvurechenskii, A. I. Nikiforov, E. Y. Zhdanov, and Y. M. Galperin, J. Phys. **25**, 505801 (2013).
[32] V. L. Nguyen, B. Z. Spivak, and B. I. Shklovsky, JETP Lett. **41**, 35 (1985).
[33] V. L. Nguyen, B. Z. Spivak, and B. I. Shklovsky, JETP **89**, 1770 (1985).
[34] B. Kochman, S. Ghosh, J. Singh, and P. Bhattacharya, J. Phys. D, Appl. Phys. **35**, L65 (2002).
[35] E. L. Nagaev, Magnetic Materials with Complex Exchange Interactions (Nauka, Moscow, 1988), p. 232.

